

Synchronous and Asynchronous Detection of Ultra-Low Light Levels

Christian Lotto^{1,3}, Peter Seitz^{2,3}

1 CSEM SA, Photonics Division, Technopark, CH-8005 Zurich, Switzerland

2 CSEM SA, Nanomedicine Division, CH-7302 Landquart, Switzerland

3 EPFL STI IMT-NE, Federal Inst. of Technology, CH-2000 Neuchâtel, Switzerland

phone: +41 44 497 1443; e-mail: christian.lotto@csem.ch

Abstract — Comprehensive analysis of noise sources in photocharge detectors leads to two novel, compact pixel circuits for ultra-low-noise light detection using optimum bandwidth engineering. A synchronous 4T CMOS image sensor pixel with in-pixel amplification reaches $0.9e^-$ readout noise, $1.5e^-$ overall noise and $300\mu\text{V}/e^-$ pixel conversion factor. An asynchronous 6T pixel for time-resolved pulse detection shows an amplitude noise of $12e^-$.

1. INTRODUCTION

The holy grail of solid state imaging is single-photon detectivity. This goal can be approached with low-noise charge detector circuits. Detector circuits generally fulfill three main functions: Transformation of photo-generated charge carriers into an electrical signal with low impedance (buffering), removal of photo-generated charge during a given period (reset), and the subsequent processing of the detected signal.

An analysis of the noise associated with the mentioned functions is performed and two novel circuits for synchronous and asynchronous detection are presented.

2. SPECTRAL PROPERTIES OF NOISE SOURCES IN DETECTOR CIRCUITS

2.1 Synchronous Detection

Synchronous detector circuits, such as conventional 4T-pixel circuits of CMOS images sensors, commonly use the correlated double sampling (CDS) technique. In this case the sampling rate f_s is twice the line rate, and the signal is modulated at half the sampling frequency. The expression below gives the modulated signal spectrum for the example of a constant illumination level:

$$signal_{sync} = \frac{1}{2} \text{sinc}\left(\frac{f}{f_s}\right) e^{-i\pi f/f_s} \sum_{n=-\infty}^{\infty} \delta\left(f - n \frac{f_s}{2}\right) \quad (1)$$

For analysis, the noisy reset level can be considered as a DC error signal:

$$n_{r, sync} = c_1 \cdot \delta(0) \quad (2)$$

The pixel buffer noise has a continuous spectrum, generally consisting of a white component and a component proportional to the inverse square root of the frequency:

$$n_{buf} = c_2 + \frac{c_3}{\sqrt{f}} \quad (3)$$

Bandwidth minimization for reset noise and buffer noise reduction is achieved by a combination of continuous-time low-pass filtering and discrete-time high-pass filtering. Low-pass filtering is usually performed naturally by the buffer and the column load capacitance. Sampling the pixel output and computing the difference of subsequent samples according to the CDS method performs the high-pass filtering. The transfer function of the resulting band-pass processing is given in equation 4. Spectra of the signal, the noise sources, and the processing transfer function are shown in figure 1.

$$H_{sync} = 2 \sin\left(\pi \frac{f}{f_s}\right) \cdot \frac{1}{1 + j \frac{f}{f_p}} \cdot e^{-\frac{\pi f}{f_s}} \quad (4)$$

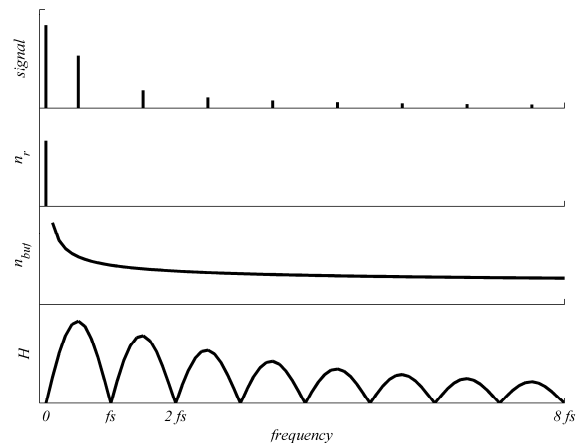


Fig. 1: Synchronous Detection: Amplitude Spectra of the Modulated Signal (for Constant Intensity), Reset Noise, Buffer Noise, and Processing Transfer Function (from top to bottom)

2.2 Asynchronous Detection

Amplitude detection and temporal discrimination of charge pulses are required for applications such as X-ray photon counting or pulsed time-of-flight ranging. Various asynchronous charge detector circuits, e.g. capacitance feedback amplifiers [1], may be used for these applications. We suggest the use of an asynchronous charge detecting circuit that includes a noise filter [2], as schematically illustrated in figure 2. The recharge resistor R_r performs a continuous-time reset of the sense node. This results in high-pass shaping of the input current signal and attenuation of pulses above a certain width. If we consider a square signal current pulse with a width of t_p and an amplitude of i_p , the spectrum of the shaped equivalent current signal is described by equation 5.

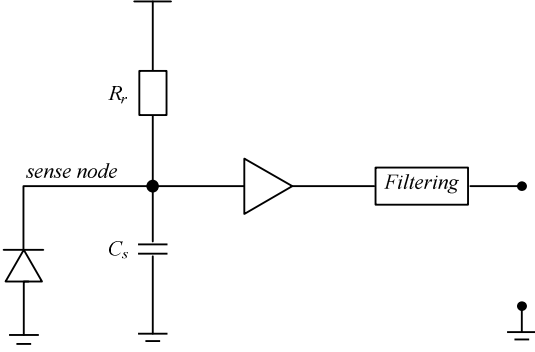


Fig. 2: Asynchronous Detection Circuit with Noise Filter

$$signal_{cur,shaped,async} = i_p t_p \text{sinc}(f t_p) \cdot \frac{j \cdot 2\pi f R_r C_s}{1 + j \cdot 2\pi f R_r C_s} \quad (5)$$

As opposed to the synchronous case, the reset noise spectrum (equation 6) has a non-zero bandwidth.

$$n_{r,async} = \sqrt{4kTR_r} \frac{1}{1 + sR_r C_s} \quad (6)$$

The buffer noise spectrum is, as in the synchronous case, a combination of white and $1/\sqrt{f}$ components. The presented detector circuit includes a filter that attenuates low frequencies for a reduction of the reset noise. A band-pass filter also suppresses high frequency components of its self-generated noise and of the buffer noise. It therefore achieves better noise performance than a high-pass filter. The transfer function of a continuous-time first order band-pass filter as used in the presented circuit is given in equation 7.

$$H_{filter} = \frac{j \cdot \frac{f}{f_l}}{\left(1 + j \cdot \frac{f}{f_l}\right) \left(1 + j \cdot \frac{f}{f_h}\right)} \quad (7)$$

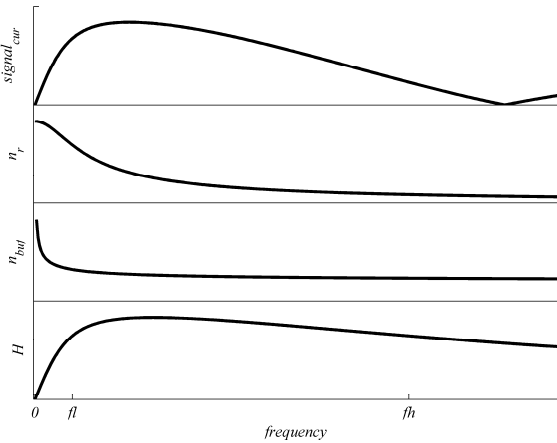


Fig. 3: Asynchronous Detection: Spectra of a Square Wave Current Pulse Signal Shaped by the Reset Resistor and the Sense Node Capacitance, Reset Noise, Buffer Noise and Band-Pass Filtering Function According to Equations 5,6,3,7 (from top to bottom)

3. IMPLEMENTED DETECTOR CIRCUITS

3.1 Synchronous Circuit

The combination of low-pass filtering and CDS, as described in paragraph 2.1, suppresses reset noise and reduces electronic noise from the buffer in synchronous detector circuits. Based on this processing method, image sensors with source-follower pixel buffers have achieved very low input referred noise floors (e.g. 2.5 electrons at common video frame rates [3]). Electronic noise from downstream circuits such as column amplifiers, output buffers, or ADCs is an important remaining noise source in these image sensors.

We propose a novel synchronous CMOS image sensor pixel with an in-pixel voltage amplifier (see figure 4) [4]. Due to amplification, the impact of electronic noise from downstream circuits is effectively reduced to a high degree. The remaining readout noise is dominated by the pixel amplifier's performance.

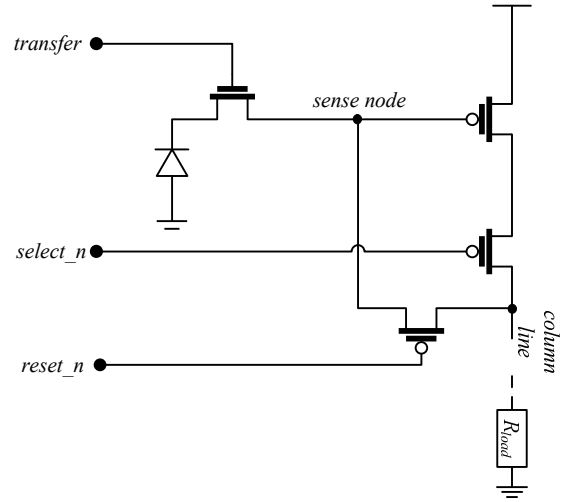


Fig. 4: Amplifying 4-Transistor-Pixel for Ultra-Low-Noise CMOS Image Sensor

The pixel is implemented using a buried photodiode and it is controlled using a standard CDS operating sequence. The select transistor is activated during all phases of the pixel readout sequence and allows the drain current of the common-source amplifier transistor to flow into a column-wise shared load resistor. During the reset phase, the reset transistor establishes a short-circuit feedback path between the input and the output of the amplifier, i.e. between the sense node and the column line respectively. During this phase, the sense node voltage is, therefore, set to a value that guarantees that the common-source transistor is in saturation. At the end of the reset phase the reset transistor is turned off and the common-source amplifier is operated in an open-loop configuration during the reset level readout. During this phase, the sense node stores the reset voltage and the common-source transistor is still saturated. The signal level readout phase is started by transferring photo-electrical charge from the buried photodiode onto the sense node. As the amplifier is still operated in an open-loop configuration during this time, the decrease of the sense node voltage leads to an amplified increase of the column voltage. For low amounts of signal charge, the common-source transistor remains saturated and nearly linear amplification at a

significant gain is obtained. However, beyond a certain amount of signal charge, the common-source transistor enters the triode operation region characterized by a continuously decreasing amplifier gain. As illustrated in figure 5, the resulting smooth compression characteristics of the amplifier can combine, without column voltage clipping, high voltage amplification at low signal levels (where readout noise will be minimized) with a wide sense node swing.

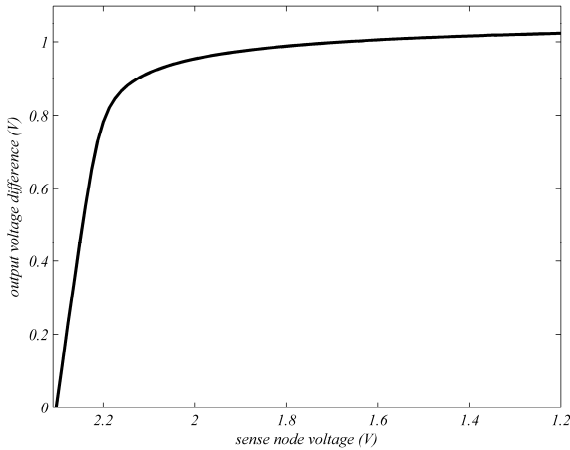


Fig. 5: Measured Open-Loop DC Characteristics of the Amplifying 4T-Pixel. The Sense Node Voltage at Reset is 2.3V.

As in the case of source-follower pixels, thermal noise of the common-source amplifier is minimized by limiting the column signal bandwidth. Compared to a source-follower with equivalent transconductance, the output impedance of a voltage amplifier is higher by the proportion of the voltage gain. A minimized column bandwidth, which matches the settling time requirements for video frame rate operation, can therefore be achieved without large column filtering capacitance. The parasitic capacitance of the column line will be sufficient in many cases.

A test chip with a small array of amplifying pixels and a simple readout chain consisting of a column multiplexer and an output driver has been designed and fabricated. An optical fill factor of 48% is achieved at a pixel pitch of 11µm. A capacitor corresponding to the parasitic capacitance of 1000 rows of pixels has been connected to each column in order to emulate the load of an array with over 1 million pixels. Readout of up to 60 000 rows/s, i.e. 60 frames/s, is possible. In the future, the shared pixel circuitry concept will help to maintain high fill factors as the pixel pitch reduces.

Measurements are performed using a discrete off-chip ADC and digital CDS. From the photon shot noise limited section of the photon transfer curve (figure 6), we can determine the overall conversion factor of 8.8 LSB/electron. Furthermore, the ratio of the ADC output the over sense node voltage is measured using a test pixel with an electrical stimulation of the amplifier input (figure 5). Combining these measurements yields a sense node capacitance of 5.3fF. From this, a pixel conversion factor of about 300µV/e⁻ is deduced.

The readout noise of each pixel has been measured using a standard readout sequence, that does not activate the transfer gate. This value therefore contains the sense node leakage current shot noise as well as the electrical noise of the output

driver and the in-pixel amplifier. The latter is the dominant readout noise contribution. Figure 7 gives the readout noise histogram of 140 pixels. The noise has been determined from the standard deviation of 500 readouts performed on each pixel at an ambient air temperature of 25°C.

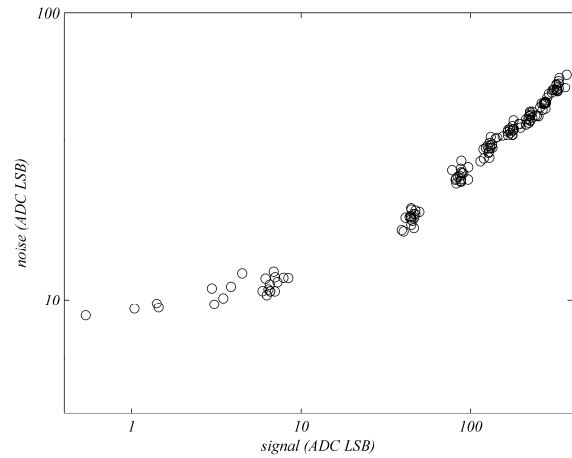


Fig. 6: Photon Transfer Curve. Exposure Time = 1ms. Overall Conversion Factor: 8.8 LSB/e⁻. Noise Floor: 1.1e⁻

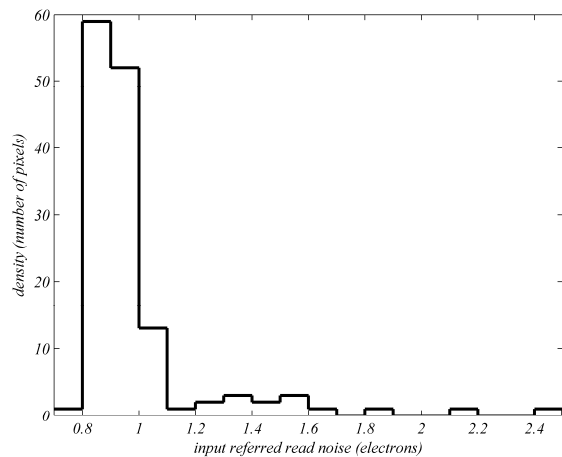


Fig. 7: Readout noise distribution for 140 pixels.

Typical pixels (median) achieve a readout noise of 0.9 electrons RMS.

The overall dark noise is found to be 1.5 electrons RMS for standard operation at an exposure time of 17ms (60 frames/s without electronic shuttering). An overall dark noise of 1.1 electrons is found when reducing the exposure time by electronic shuttering to 1ms. From these measurements, an estimate of the photodiode dark current shot noise of 1.0 electrons RMS at 17ms exposure time is found. Furthermore, a noise component of 0.6 electrons, associated with the operation of the transfer gate but independent of the exposure time, is observed. This noise component is believed to be charge transfer noise as described by Fowler et al. [5].

The readout noise histogram contains some pixels with values noticeably higher than the main peak of the distribution. Detailed investigation of the output waveforms indicates that the concerned pixels suffer from the Random Telegraph Signal (RTS) effect due to single electron trapping in the gate oxide of the common-source transistor as reported by Wang et al. [6].

A full well capacity of $34ke^-$ has been measured. Dynamic range values of 87.1dB and 89.8dB are therefore found at exposure times of 17ms and 1ms respectively.

3.1 Asynchronous Circuit

A compact pixel circuit implementation (see figure 8) of the novel asynchronous charge detecting circuit, as discussed in paragraph 2.2, has been designed. A simple source-follower is buffering the sense node signal. The continuous-time band-pass filter consists of a passive first order high-pass filter followed by a source-follower with a load capacitance. MOS transistors are used as implementations of the reset resistor as well as the resistor of the high-pass filter.

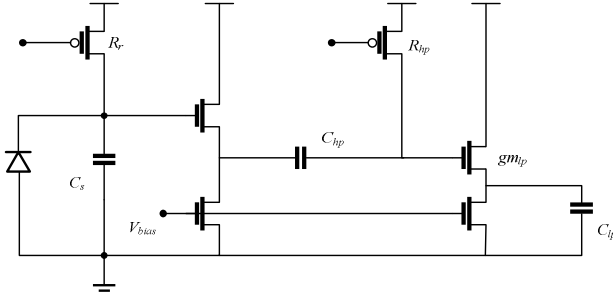


Fig. 8: Schematic of the Asynchronous Detection Pixel

The minimum lower band-limit $f_1=1/(2\pi R_{hp}C_{hp})$ of the filter is defined by the maximum signal pulse width to be detected. For effective reduction of reset noise, it is important to keep the bandwidth of the reset noise significantly below f_1 . A high value of the reset resistance R_r is therefore required. An approximate expression of the reset noise component after band-pass filtering is given in equation 8. Figure 9 plots the spectrum of the reset noise on the sense node and of the filtered reset noise. A simple estimation of the filtered reset noise voltage is given in equation 9. The degree of reset noise suppression is proportional to the square root of the ratio of the reset noise bandwidth over the lower limit of the band-pass filter.

$$n_{out,r} \cong \sqrt{4kTR_r} \left(\frac{1}{1 + j2\pi f R_r C_s} \cdot \frac{j2\pi f R_{hp} C_{hp}}{1 + j2\pi f R_{hp} C_{hp}} \cdot \frac{1}{\left(1 + j2\pi f \frac{C_{lp}}{gm_{lp}}\right)} \right) \quad (8)$$

$$v_{n,Rr} \leq \sqrt{\frac{R_{hp} C_{hp}}{R_r C_s} \frac{kT}{C_s}} \quad (9)$$

Note that the filtering suppresses some low frequency content of the signal spectrum (equation 5). However, this does not affect the detection of the signal pulses as the relevant information, such as the arrival time and the signal charge amount, are residing in higher frequency ranges of the signal spectrum.

The optoelectronic transducer of the implemented pixel circuit is a drift-field-enhanced photogate with a sense node capacitance of 10fF. The resistor R_{hp} of the high-pass filter is tunable. The reset noise component can be reduced by increasing the high-pass filter frequency f_1 (measurements in figure 10). The dominant contributions in the asymptotic noise level are buffer noise and self-generated noise of the

filter. Light pulses with a width of 1 μ s and a repetition rate of 5000/sec are detected at a noise level of 12 electrons.

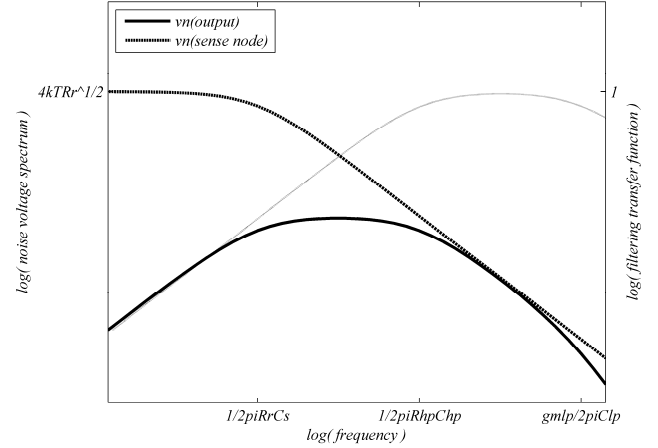


Fig. 9: Asynchronous Circuit: Reset Noise Spectrum on the Sense Node, Spectrum of the Reset Noise Component on the Output Node

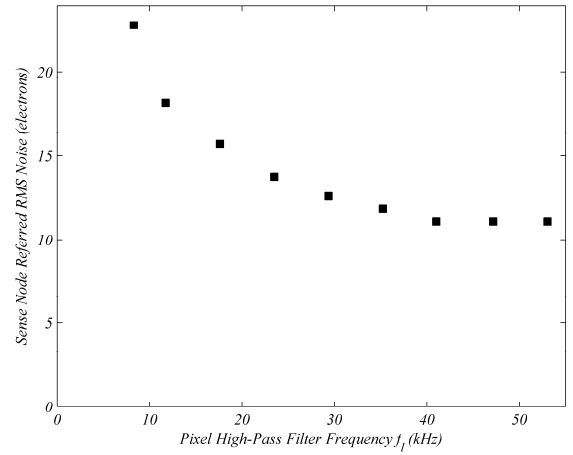


Fig. 10: Measured Overall Noise vs. High-Pass Filter Frequency

4. CONCLUSION

Bandwidth engineering allows the reduction of both reset and buffer noise in detection circuits.

In circuits with an asynchronous reset, the reset noise is efficiently reduced to $12e^-$ by the narrow-bandwidth shaping and high-pass filtering of the reset noise.

The developed synchronous amplifying 4T CMOS image sensor pixel achieves a $0.9e^-$ sensor readout noise and an overall noise of $1.5e^-$ or less due to its high pixel conversion factor and optimized bandwidth reduction.

REFERENCES

- [1] G. Lutz, "Semiconductor Radiation Detectors", Springer, Berlin, 2007.
- [2] C. Lotto and P. Seitz, "Charge Pulse Detecting Circuit", EP Patent Application No. EP 08169759.1, 2008.
- [3] S. Neukom *et al.*, "A Low-Noise CMOS Imager with $1.2e^-$ Readout Noise, $2.5e^-$ Overall Noise and over 140dB Dynamic Range at 60fps", EOS Conference on Frontiers in Electronic Imaging, Munich, Germany, June 15-17, 2009.
- [4] C. Lotto and P. Seitz, "Single Photon Detector Imaging Device", EP Patent Application No. EP 08163384.4, 2008.
- [5] B. Fowler *et al.*, "Charge Transfer Noise in Image Sensors", in Proc. 2007 International Image Sensor Workshop, Ogunquit Maine, USA, June 7-10, 2007.
- [6] X. Wang *et al.*, "Random Telegraph Signal in CMOS Image Sensor Pixels", pp. 115-118, International Electron Devices Meeting, 2006.